Environmental DNA

WILEY

Environmental DNA
Open Access
Dedicated to the study and use of environmental DNA for basic and applied sciences

ORIGINAL ARTICLE OPEN ACCESS

Filtering Microbial Diversity: Evaluation of Different Pore Sizes for eDNA Community Profiling

Irene Gregori[1,2] | Francesco Martino[1] | Lorenzo Zane[1,2,3] | Alberto Pallavicini[2,4,5] | Alessandro Vezzi[1,2]

[1]Department of Biology, University of Padova, Padova, Italy | [2]National Biodiversity Future Centre (NBFC), Palermo, Palermo, Italy | [3]Consorzio Nazionale Interuniversitario per le Scienze del Mare (CoNISMa), Roma, Roma, Italy | [4]Department of Life Sciences, University of Trieste, Trieste, Italy | [5]National Institute of Oceanography and Applied Geophysics - OGS, Trieste, Italy

Correspondence: Lorenzo Zane (lorenzo.zane@unipd.it)

Received: 10 July 2025 | **Revised:** 8 October 2025 | **Accepted:** 16 October 2025

Funding: This work was supported by European Union NextGenerationEU (PNRR CN_00000033, PNRR ECS_00000043) and Ministero dell'Università e della Ricerca (PRIN 2020 Prot. 2020J3W3WC).

Keywords: eDNA | filter pore size | holistic monitoring | microbial metabarcoding

ABSTRACT

Environmental DNA (eDNA) metabarcoding is widely used in biodiversity monitoring, and its popularity is also growing because of its potential to simultaneously detect multiple taxonomic groups, allowing holistic community assessments. When working with water samples, the choice of the filter type is one of the key methodological factors influencing community characterization, with 0.22 μm pore size filters typically used for microbial communities and larger filters for eDNA of larger organisms. However, as holistic community assessments are increasingly adopted, the use of a single filter pore size would help to optimize sampling and experimental efforts. Yet, it remains unclear whether filters with large pore sizes can effectively capture both microbial and macro-organism eDNA. This study evaluates the use of 0.45 μm filters, commonly used for metazoan eDNA metabarcoding, in assessing microbial diversity across different coastal environments. Replicates of water samples from the Venice Lagoon and nearby waters were filtered independently using both 0.45 μm and the standard 0.22 μm pore size filters and analyzed through 16S rRNA gene metabarcoding. Both filters capture a shared core microbial community, but they also retain distinct taxa. Alpha diversity was significantly higher in samples collected with the 0.45 μm filters, which also showed a more effective recovery of particle-associated microbes. Our work contributes to optimizing eDNA-based methodologies for large-scale multi-taxa biodiversity monitoring, demonstrating that 0.45 μm filters can effectively capture microbial diversity and supporting their use in holistic studies in aquatic environments.

1 | Introduction

Environmental DNA (eDNA) metabarcoding revolutionized biodiversity monitoring, outperforming traditional methods such as visual surveys, manual collection, and morphological identification, allowing the assessment of large-scale biodiversity data (Fediajevaite et al. 2021). Pioneering studies of microbial diversity and evolution (Olsen et al. 1986; Pace et al. 1986) gave rise to the field of molecular microbial ecology and reshaped our understanding of microbial biodiversity and its significance. After more than two decades, molecular approaches for detecting individual species or characterizing communities from environmental samples have been extended to macro-organisms (Ficetola et al. 2008; Pompanon et al. 2012; Sønstebø et al. 2010). With the rapid expansion of eDNA metabarcoding studies in recent years, the focus has shifted from single target groups such as fish (Cananzi et al. 2022) or invertebrates (Klymus et al. 2017; Martino et al. 2025) to a more comprehensive assessment of the

entire ecological community in the so-called holistic or "tree of life" studies (Djurhuus et al. 2020; Ficetola and Taberlet 2023; Xu et al. 2023). By integrating information from multiple levels of biodiversity, ideally starting from a single sample, this latter approach aims at the identification of entire communities within an environment—from microbes to larger organisms (Coble et al. 2019; Miya 2022; Zhang et al. 2020)—supporting comprehensive ecosystem evaluations, useful to reveal species co-occurrence patterns across taxonomic domains and their shifts in response to environmental changes (Cook et al. 2025).

When eDNA is collected from water samples, it would be preferable to perform holistic assessments using a single type of filter capable of capturing eDNA of different organisms, avoiding repeated filtration and ensuring that all taxonomic groups are analyzed from the same water sample. The need for optimization becomes even more relevant as eDNA metabarcoding is increasingly adopted as a standard tool for wide biodiversity monitoring (Collins et al. 2022; Deiner et al. 2017; He et al. 2023; Taberlet 2018) thanks to its ability to assess ecosystems across vast spatial scales and over extended temporal periods. In fact, many recent studies have implemented large sampling designs, covered diverse habitats and spanned long time series, to track changes in biodiversity and ecosystem health (Bohmann et al. 2014; Deiner et al. 2017).

Expanding the spatial and temporal scale of surveys makes biodiversity monitoring more valuable and informative, but also introduces significant logistical and financial challenges. In fact, although metabarcoding is often more cost-effective than traditional methods (Fu et al. 2021), its large-scale implementation still requires substantial resources, including laboratory reagents, sequencing costs, and considerable time and personnel commitments. Reducing sampling effort—for example, by using a single filter type for multiple applications—could help lower these costs by minimizing both fieldwork and nucleic acid extraction requirements, thus enhancing the feasibility of eDNA-based monitoring for long-term, large-scale ecological studies. The use of a single filter in holistic studies would also reduce stochasticity and contamination risks, as just one water sample is used to characterize the entire community.

Although using a single filter type would be advantageous, it remains unclear which one would be most appropriate, as most metabarcoding studies on water samples have relied on filters with different pore sizes: 0.22 μm filters are commonly used for microbial DNA sampling (Galand et al. 2018; Gifford et al. 2011), while larger pore sizes, such as 0.45 μm are typically employed for capturing eukaryotic eDNA—including that of macro-organisms—in marine and transitional ecosystems (Aglieri et al. 2021; Blabolil et al. 2021; Cananzi et al. 2022; Martino et al. 2025; Nguyen et al. 2020; Pinna et al. 2024). However, the suitability of 0.45 μm filters has not been comprehensively assessed across diverse aquatic environments for microbial diversity characterization using 16S rRNA gene metabarcoding. In fact, previous studies have explored various aspects of eDNA metabarcoding, including sequencing platforms, amplification protocols, and extraction methods (Brandt et al. 2021; Goldberg et al. 2016; Hering et al. 2018), yet filter type remains a comparatively understudied factor, particularly regarding the suitability of 0.45 μm filters for microbial community characterization. If proven effective, a single filter type could recover both micro- and macro-organism eDNA, potentially simplifying sampling protocols and improving the efficiency of biodiversity monitoring efforts.

Here, we address this issue by assessing the effectiveness of 0.45 μm pore size filters for microbial community analysis. Water samples from different environments in and in the waters nearby the Venice Lagoon were filtered using both 0.22 μm and 0.45 μm pore size membranes, and, after eDNA extraction, amplification, and sequencing, the metabarcoding data obtained using the different filters were compared. Specifically, this study aims to: (1) Evaluate the suitability of the 0.45 μm filter for detecting microbial communities in water samples; (2) Assess whether the microbial communities detected using the 0.45 μm and 0.22 μm filters differ significantly, making the structure of the communities obtained substantially different; (3) Investigate whether the observed differences between the two filters are influenced by environmental parameters, potentially shaping the microbial diversity detected. To address these questions, we integrate taxonomic analyses, ordination methods, and diversity indices to evaluate the impact of pore size on microbial community detection and assess whether this effect varies across environments with different ecological conditions.

2 | Materials and Methods

2.1 | Site Selection and Sampling

Four different sampling sites were selected in the Venice Lagoon and the adjacent sea (Figure 1) to represent different environmental conditions: a tidal channel in a natural salt marsh (NATS), one in an artificial salt marsh (ARTS), a site within the Chioggia Inlet (CHIN), and a site outside the lagoon, near the Chioggia Inlet (CHOU). These sites are characterized by different environmental parameters (see Table S1 for the sites inside the lagoon), such as nutrient concentration and salinity, that may influence the characterization of microbial communities. The salt marsh sites (ARTS and NATS) are located in tidal channels with an average water depth of approximately 30 cm. These environments are typically rich in nutrients that have a key role in supporting the growth and productivity of salt marsh vegetation and microbial communities (Carmona et al. 2021). Examples include phosphorus (P), silicon (Si), and nitrogen (N), primarily found as ammonium (NH4+), the most abundant nitrogen form in these ecosystems. At the other sites, the water is deeper, reaching 10 m at the CHIN site and 12 m at the CHOU site. The CHIN site is very close to the Chioggia Inlet, one of the three openings connecting the Venice Lagoon to the Adriatic Sea, and it is therefore characterized by more marine conditions, with lower nutrient concentrations, higher salinity, and less turbid waters. Finally, the CHOU site is located just outside the Venice Lagoon, and it is characterized by fully marine conditions.

The exact locations of the sampling sites are shown in Figure 1, with detailed information in the figure caption.

In spring 2023, surface water was collected in pre-cleaned tanks and immediately filtered with a portable vacuum pump (eDNA Citizen Scientist Sampler, Smith-Root) using two

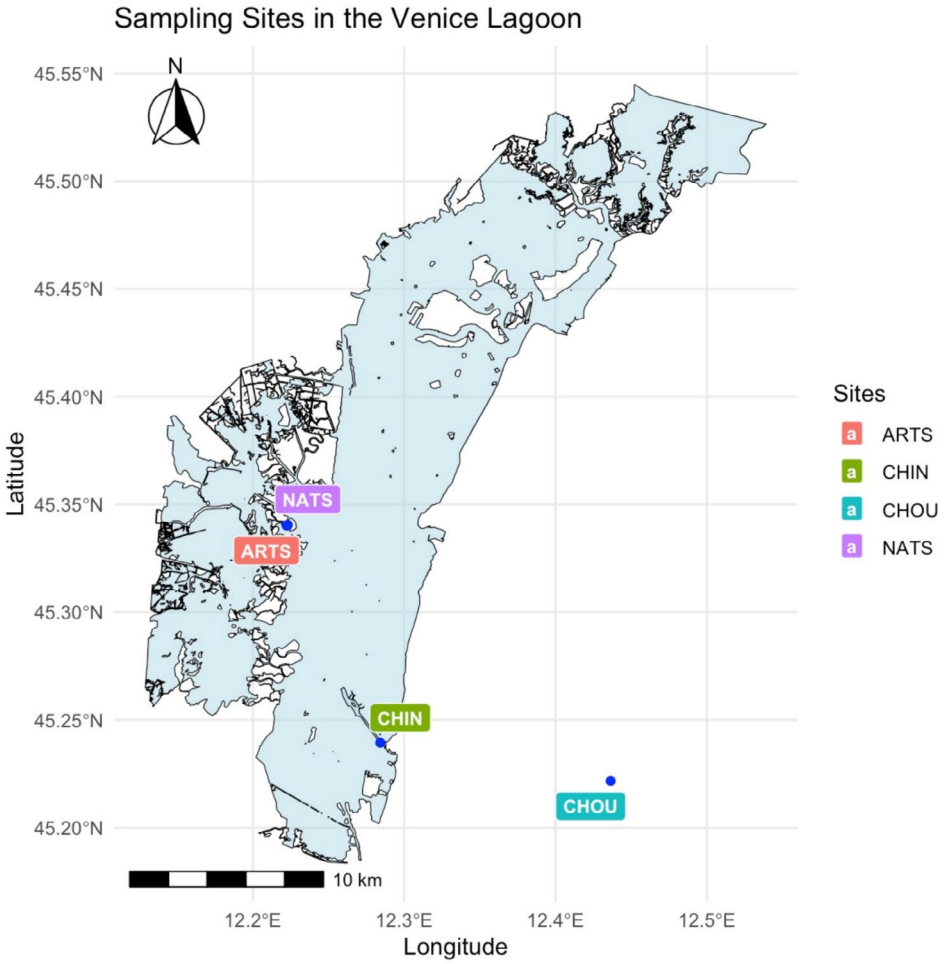

FIGURE 1 | Map of the Venice lagoon with the sampling points (blue dots). Water samples were collected from the tidal channels of the two salt marshes (NATS 45°20′26" N—12°13′23" E and ARTS 45°20′25" N—12°13′20" E), one site inside the Chioggia inlet (CHIN 45°14′22" N—12°17′03" E), and one outside the lagoon (CHOU 45°13′18" N—12°26′1" E).

different pore-size PES membranes: 0.45 μm (Smith-Root) and 0.22 μm (Merck Millipore). In detail, two separate 2 L aliquots were taken from the same tank and filtered independently, one with a 0.45 μm membrane and the other with a 0.22 μm membrane. This procedure ensured that each 0.45 μm filter had a corresponding 0.22 μm filter for comparison, avoiding sequential filtration, since they both filtered the same volume of water from the same tank. Gentle shaking of the water was performed prior to each filtration step to ensure proper mixing. All filters (47 mm in diameter) had identical surface areas, maintaining a consistent volume-to-surface area ratio across replicates. As a result, three replicates per filter type were obtained at each site, for a total of 24 filters: 12 with 0.45 μm membranes and 12 with 0.22 μm membranes, obtaining a balanced and comparable dataset.

2.2 | DNA Extraction and Sequencing

DNA was extracted from each filter using two different extraction kits: the DNeasy Blood and Tissue Kit (Qiagen) and the PowerWater DNA Isolation Kit (Qiagen), following the manufacturer's instructions. This approach was used to evaluate potential differences in the performance of the two extraction methods. This resulted in a total of 48 samples, with details provided in Table S2. DNA quality and quantity were assessed using a Nanodrop spectrophotometer (Thermo Fisher Scientific), and all samples met the minimum quality and quantity requirements for amplification. The V4-V5 region of the 16S rRNA gene was amplified in triplicate using primers 515-Y (5′-GTGYCAGCMGCCGCGGTAA-3′) and 926R (5′-CGYCAATTYMTTTRAGTTT-3′) (Parada et al. 2016) through a two-step PCR protocol incorporating Illumina indexes. Libraries were prepared following the 16S Metagenomic Sequencing Library Preparation protocol (Illumina 2013) and sequenced on an Illumina MiSeq platform (2 × 300 bp reads) at BMR Genomics Srl (Padova).

2.3 | Data Analyses and Visualization

Raw sequencing data quality was assessed using FastQC (Andrews 2010). Sequences were filtered with Cutadapt (Martin 2011) and analyzed using QIIME2 v2024.10 (Bolyen et al. 2019). Sequence denoising, trimming, and chimera removal were performed with DADA2 (Callahan et al. 2016). Taxonomic

assignment was conducted using a Naïve Bayes classifier, pre-trained on the Silva database version 138.2 (Quast et al. 2012), clustered at 99% similarity at the genus level.

Exploratory and statistical analyses were performed in R (v4.0.3, R Core Team, 2019). Rarefaction curves were generated using the rarecurve function from the *vegan* package (Oksanen et al. 2001) to evaluate sequencing depth and biodiversity coverage to possibly exclude some samples. Sample completeness then was quantitatively assessed also using the *iNEXT* package (Hsieh et al. 2016) with the function "estimateD (assemblages_list, q = 0, datatype = "abundance", base = "size")" (Chao et al. 2014). The default threshold of SC ≥ 0.985 was applied, corresponding to samples capturing at least 98.5% of the estimated community. To account for differences in sequencing depth across samples, data normalization was applied using the function "rarefy_even_depth (ps, sample.size = min(sample_sums ps)), rngseed = 123, replace = FALSE" of the *phyloseq* package (McMurdie and Holmes 2013). We selected rarefaction as the normalization approach as recommended by previous studies (McKnight et al. 2019; Weiss et al. 2017), since it is the most appropriate method for ecological community studies with large differences in sequencing depth, and it helps minimize false positives in ecological comparisons. Differences in microbial community composition were tested with a permutational multivariate analysis of variance (PERMANOVA) using the adonis2 function of the *vegan* package in R. The analysis was performed on a distance matrix calculated from microbial community data, using Bray-Curtis dissimilarities. The initial PERMANOVA with 4999 permutations was conducted with the function "adonis2(dist_matrix ~ pore + extraction + site, by = "terms")", where "pore", "extraction", and "site" were treated as independent variables. Given that "site" and "pore" were highly significant (see Results), additional analyses were performed to clarify their respective contributions. Specifically, the dataset was stratified by "site", and separate PERMANOVA tests were conducted within each site to assess the effect of "pore" while controlling for site-related variation. We also tested for homogeneity of multivariate dispersions (Anderson 2006) using Bray–Curtis distances, to evaluate whether filters differed in the variability of community profiles across replicates. In this case, differences between filters were assessed using ANOVA, followed by Tukey's HSD for pairwise comparisons.

To quantitatively compare the microbial taxa detected with different pore sizes (0.45 μm and 0.22 μm) across sites, Venn diagrams were generated. ASVs present in at least one sample were extracted from the phyloseq object and grouped by pore size. Overlapping and unique ASVs were visualized using the *VennDiagram* package in R (Chen and Boutros 2011). To also provide qualitative information, microbial relative abundance across the samples was analyzed at the phylum level.

Relative abundances of taxa were calculated, and the 10 most abundant phyla were selected. Mean values were calculated for each site and pore size. To account for variation across phyla, values were row-scaled using a Z-score transformation, centering each phylum's abundance around zero. To visualize the results, a heatmap was generated using the *pheatmap* package in R (Kolde and Kolde 2015), with column annotations indicating pore size, which were color-coded accordingly, and columns grouped by site.

Beta diversity was assessed using Bray–Curtis dissimilarity matrices, calculated with the vegdist function (*vegan* package), and PCoA ordinations were generated using the capscale function (*vegan* package) to visualize differences in microbial community structure. The contribution of the most influential ASVs annotated at the genus level (or family if genus was unavailable) was represented as vectors overlaid on the ordination plots. The 10 most influential ASVs were identified based on the highest sums of the absolute values of their coordinates on the first two PCoA axes (PC1 and PC2).

Alpha diversity was measured using the Shannon index, calculated with the estimate_richness function (*phyloseq* package). Differences between pore sizes were tested using the Kruskal–Wallis test. Violin plots, combined with box plots, were generated using the *ggplot2* package (Gómez-Rubio 2017) to illustrate the distribution of diversity values across pore sizes, with statistical annotations added where applicable.

Finally, to further investigate the small but significant effect (see Results) of the different extraction methods, alpha diversity and taxonomic overlap (Venn diagrams) analyses were also carried out separately for the two extraction kits.

3 | Results

3.1 | Sequencing Results

The MiSeq 2 × 300 bp sequencing produced an average of 133,393 raw reads per sample. One sample contained no reads and has therefore been excluded from the analysis. The remaining samples ranged from 25,529 to a maximum of 321,755 reads. Most samples reached a plateau in the rarefaction curve analysis, indicating sufficient sequencing coverage, while pwf-01 and fbt-14 failed to reach a clear plateau (Figure S1) and were discarded. Specifically, pwf-01 was excluded because it contained less than 1500 reads, and fbt-14 was excluded because it did not meet the required completeness threshold (SC = 0.981; see Methods). To ensure robust comparisons, the corresponding paired samples with the other pore size filter (pwf-02 and fbt-13) were also excluded, leading to a final dataset of 44 samples (Table S2).

3.2 | Taxonomic Assignment and PERMANOVA Results

After taxonomic assignment, a total of 480 ASVs were detected. Of these, 106 were excluded as singletons and 6 were removed due to their taxonomic classification: Family == "Mitochondria" ($n = 1$) or Order == "Chloroplast" ($n = 5$). This resulted in 368 ASVs being retained for further analysis, as they represented the most reliable dataset. Following normalization, 43 ASVs were removed because they were no longer present in any sample after random resampling, leaving a final dataset of 312 ASVs for analysis.

The overall PERMANOVA revealed that both "site" and "pore" had a significant and strong effect on microbial community composition, whereas the variable "extraction" had a weaker yet still significant effect. The "pore" variable had a strong and significant effect ($R^2 = 0.142$, $p = 0.0002$), but the "site" variable explained the largest proportion of variance ($R^2 = 0.369$) with a significance of $p = 0.0002$, indicating strong spatial structuring of microbial communities. "Extraction" also showed a statistically significant effect ($p = 0.0302$), but its contribution to the overall variance was minimal ($R^2 = 0.031$); this weaker signal was further investigated, revealing that the significant effect was limited to the CHOU site, as displayed in the supplementary PCoA plot (Figure S4). Analyses performed on datasets divided by extraction method confirmed the same patterns observed in the overall dataset and reported below. As this investigation fell outside the main objectives of the study, the corresponding results were not detailed in the main text, but are presented in the Supporting Information (Figures S3 and S5),

TABLE 1 | Summary of the PERMANOVA analyses performed on microbial community compositions at each site separately, based on Bray–Curtis dissimilarities with 999 permutations.

Site	Variable	R^2	F-statistic	*p*
NATS	pore	0.28459	31.825	0.078
ARTS	pore	0.24606	32.636	0.011*
CHIN	pore	0.72534	21.127	0.006**
CHOU	pore	0.21490	27.373	0.112

Note: The table reports R^2 values, F statistics, and *p*-values. * and ** indicate significant results ($p \leq 0.05$ and $p \leq 0.01$, respectively).

and given that the site emerged as the strongest driver of community variation, subsequent analyses were performed separately for each site to account for site-specific variability. The results of the within-site PERMANOVA analyses, reported in Table 1, showed that "pore" variable had a significant effect in two of the four sites. The strongest effect was observed in CHIN, while ARTS also exhibited a significant, though less pronounced, effect. In contrast, no significant effect of "pore" was found in CHOU. These results indicate that the impact of the filter used on microbial community composition varies across locations, with some sites showing clear differentiation due to pore sizes, while others do not.

The multivariate dispersion test indicated a significant difference between filter types ($F = 6.31$, $p = 0.016$), with the 0.45 μm samples showing a lower dispersion around group centroids compared to 0.22 μm samples (Tukey HSD, $p = 0.016$).

3.3 | Differences in Taxa Detection

As shown in Figure 2, differences in taxa detection were observed between the two filter types, but with a substantial overlap present across all samples. The Venn diagrams summarize the differences in the number of ASVs between the two filters: the shared ones ranged from 57 to 80 (Figure 2a–d), whereas the number of unique ASVs detected varied between filter types, with the 0.22 μm filters capturing between 23 and 37 unique ASVs and the 0.45 μm filters detecting between 22 and 65 unique ASVs. Overall, across the entire dataset, 157 ASVs were shared between both filters, whereas 91 and 64 ASVs were uniquely recovered by the 0.45 μm and 0.22 μm filters, respectively

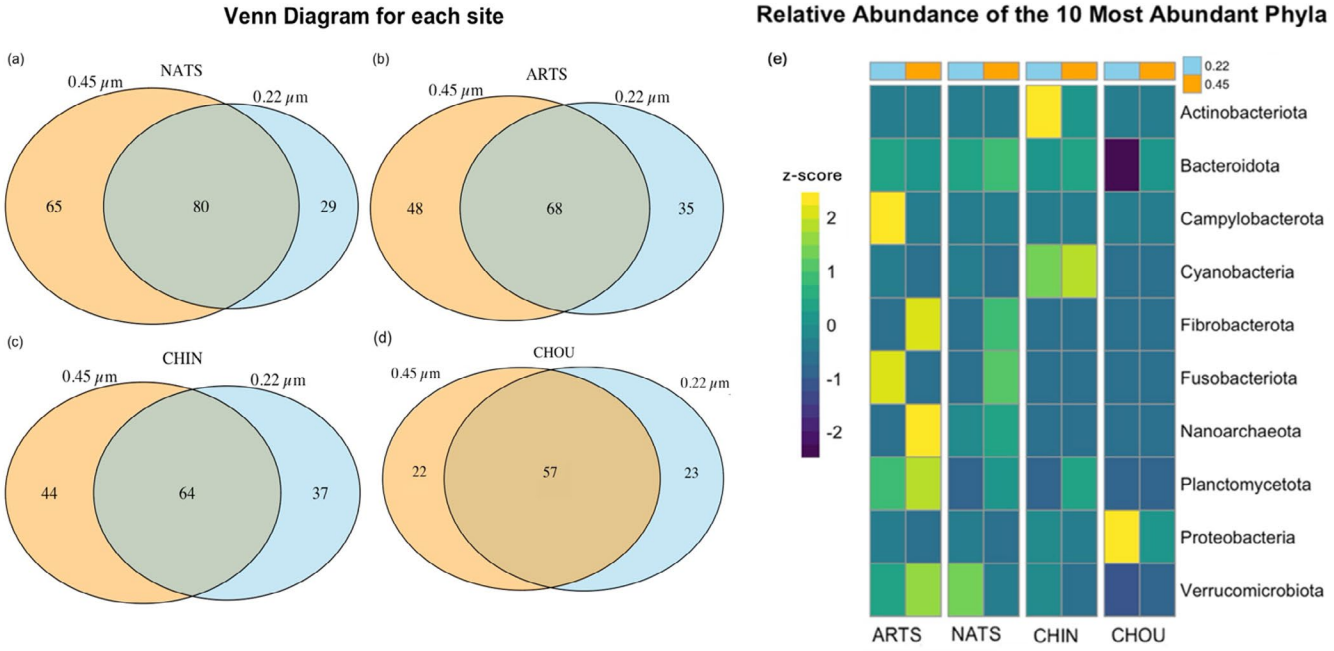

FIGURE 2 | (a-d) Venn diagrams illustrating the number of microbial taxa identified in water samples collected from four sites (ARTS, NATS, CHIN, CHOU), based on their detection through the two filters with pore sizes of 0.45 μm (orange) and 0.22 μm (light blue). (e) Heatmap showing the z-score transformed relative abundance of the top 10 most abundant microbial phyla across the four sites and the filters with different pore sizes. Each row represents a phylum, while columns are grouped by site and filter type. The z-score (from +2 to −2) highlights differences relative to the mean for each phylum, with positive values (yellow) indicating higher-than-mean abundance and negative values (blue) indicating lower-than-mean abundance. Filters with different pore sizes are color-coded above the heatmap, as in the Venn diagrams.

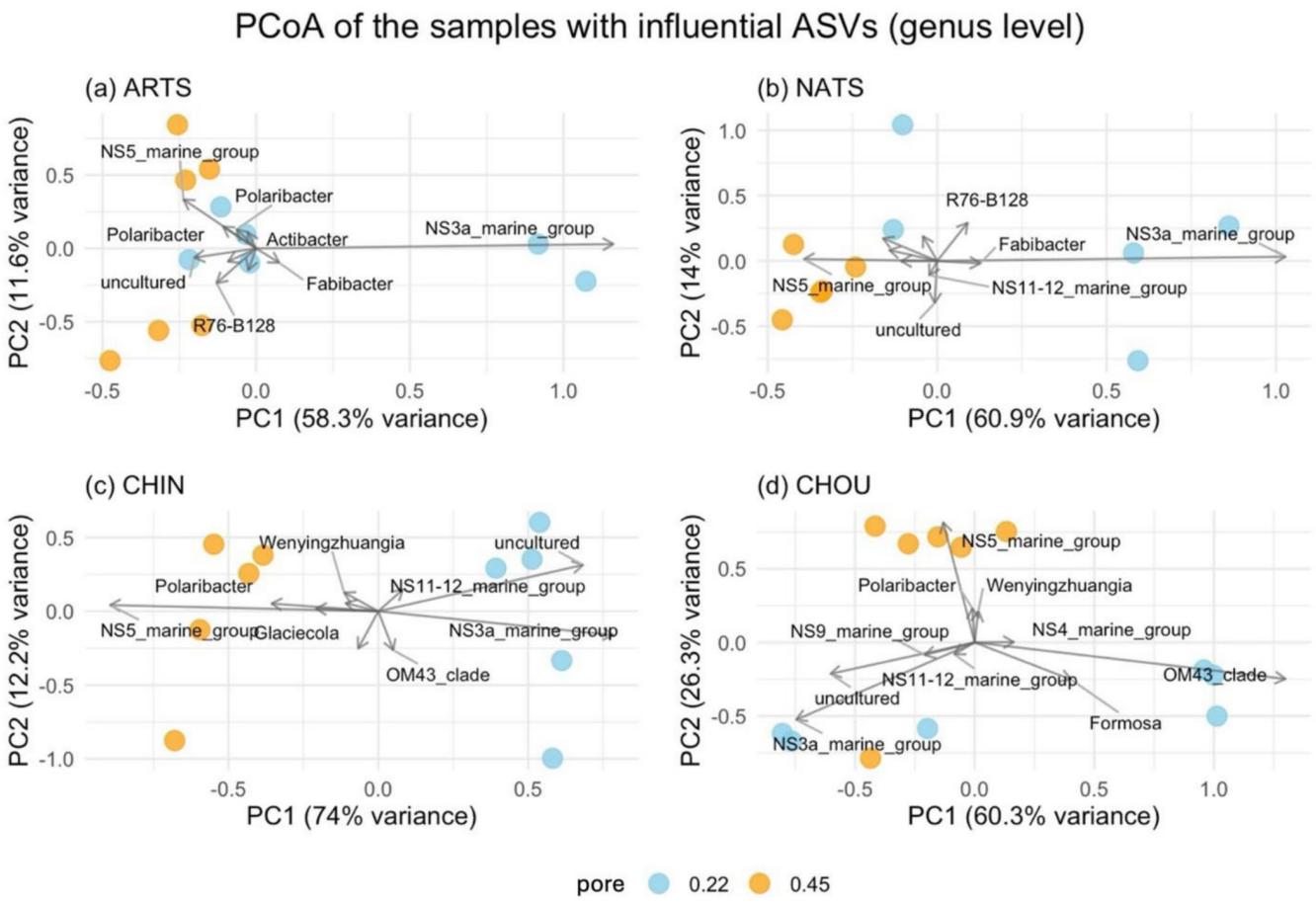

FIGURE 3 | PCoA of the samples divided by site: (a) ARTS, (b) NATS, (c) CHIN, and (d) CHOU. Points represent microbial communities characterized using filters with pore sizes of 0.22 μm (light blue) and 0.45 μm (orange), while arrows indicate the most influential genera driving the separation, which are those with the highest contributions to the variation along the first two axes.

(Figure S2). When considering the variation between sites, in three out of four cases, the 0.45 μm filters consistently recovered more ASVs than the 0.22 μm filters. In line with the non-significant result of the previous PERMANOVA analysis, the Venn diagram highlights a higher proportion of shared taxa between pore sizes at the CHOU site compared to the others.

Regarding the taxa detected by the two filters, the heatmap in Figure 2e shows the distribution of the 10 most abundant phyla across the four sampling sites and filter types (0.22 μm and 0.45 μm), based on z-scores, calculated on the mean reads abundance of each phylum across all samples, meaning that positive values indicate that a phylum is more abundant in a sample than its overall mean abundance, while negative values indicate lower-than-mean abundance. Taxonomic composition varied with both site and filter pore size. The 0.22 μm filters detected higher abundances of *Campylobacterota* (ARTS) and *Proteobacteria* (CHOU), whereas the 0.45 μm filters were more effective in detecting *Fibrobacterota* (in both marsh sites), as well as *Verrucomicrobiota*, *Nanoarchaeota*, and *Planctomycetota* (ARTS). Some phyla, such as *Fusobacteriota*, *Fibrobacterota*, and *Nanoarchaeota*, were equally represented by both filters at sites where the water was deeper (CHIN and CHOU) but showed notable differences in the marsh environments. *Bacteroidota* was completely absent in CHOU analyzed with the 0.22 μm filter and, together with an outlier pattern in *Proteobacteria*, represents an exception in an otherwise more homogeneous site compared to the others, providing additional support for the PERMANOVA results, which indicated that the filter pore size was not a significant variable in this site.

3.4 | PCoA

The PCoA plots (Figure 3) illustrate the distribution of microbial communities sampled using 0.22 μm and 0.45 μm filters across the four sites: ARTS, NATS, CHIN, and CHOU. Vectors represent the most influential microbial genera contributing to the separation of samples based on pore size. As previously observed, the two filters capture overlapping but distinct microbial communities, and the principal coordinates explain a substantial proportion of the variance. In ARTS, most samples grouped closely regardless of filter type, but a few 0.22 μm samples shifted along PC1 (58.3% variance), with the *NS3a marine group* appearing as the main contributor to this separation. A stronger separation was observed in NATS, with PC1 explaining 60.9% of the variance and PC2 14%; *NS11-12 marine group* and *NS3a marine group* were more associated with the 0.22 μm filter, while *NS5 marine group* was more represented in the 0.45 μm fraction.

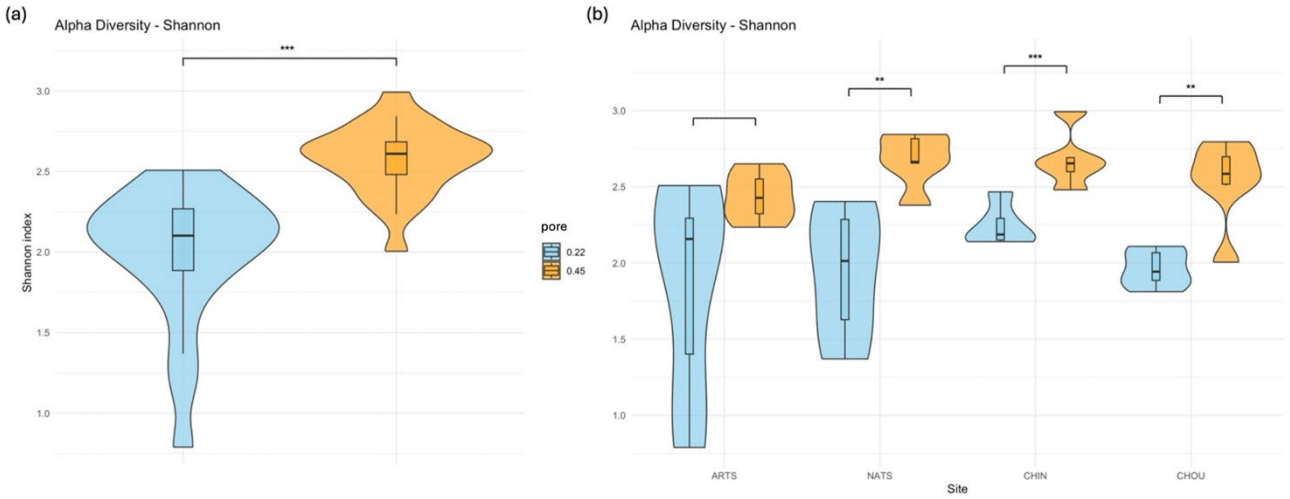

FIGURE 4 | (a) Violin plot of Shannon diversity index, comparing microbial diversity captured by 0.22 μm (light blue) and 0.45 μm (orange) filters in the overall dataset. (b) Violin plot of Shannon diversity index across the four sampling sites (ARTS, NATS, CHIN, CHOU) for both filter types. The width of each violin represents the density distribution of Shannon index values, with wider sections indicating more frequent values. The boxplot inside the violin displays the interquartile range (IQR, 50% of the data), the horizontal line represents the median, and whiskers extend to the 95% confidence interval (95% CI) or 1.5 × IQR from the quartiles. Significant differences ($p < 0.05$, Kruskal–Wallis test) are indicated with a different number of asterisks (** indicate $p < 0.01$ and *** indicate $p < 0.001$).

CHIN showed, also visually, a pronounced filter effect, with PC1 accounting for 74% of the variance. *Glaciecola* and *NS5 marine group* were enriched in the 0.45 μm fraction, while *NS3a marine group* and *NS11-12 marine group* were more prevalent in the 0.22 μm samples.

In CHOU, PC1 explained 60.3% of the variance and PC2 26.3%; *NS5 marine group* was strongly associated with the 0.45 μm filter, while *NS3a marine group*, *OM43 clade*, and *Formosa* were more abundant in the 0.22 μm fraction.

In addition to the differences observed between filters with different pore sizes, the PCoA highlights site-specific variations in microbial community composition. CHIN exhibited the most pronounced separation between the two filters, with a clear clustering pattern along PC1 (74% variance), indicating that most of the variation in microbial communities at this site is driven by filter type. This is consistent with the PERMANOVA result, which showed a high R^2 value (0.725), suggesting that filter pore size explains most of the observed variation at CHIN.

CHOU also showed a distinct filter-driven separation, particularly along PC1 (60.3% variance), but with a more pronounced spread along PC2 (26.3%), indicating additional variability within the microbial communities. In line with the PERMANOVA results indicating no significant differences between the two pore sizes at the CHOU site, samples of each filter type are separated along the second principal component, which accounts for only 26.3% of the variation. In contrast, in the other sites, the separation between filters occurs primarily along PC1—the component explaining the largest proportion of variance—further supporting the significant effect of pore size detected by PERMANOVA.

3.5 | Alpha Diversity Indices

Microbial alpha diversity significantly differed between the two filter pore sizes when considering the whole dataset. The Shannon index was significantly higher for samples collected with the 0.45 μm filter, as confirmed by the Kruskal-Wallis test ($p < 0.001$*). The violin plot (Figure 4a) clearly shows that the 0.45 μm filter captured microbial communities with consistently higher diversity, with values ranging from 2 to 2.99. In contrast, the 0.22 μm filter showed lower overall diversity (from 0.7 to 2.5) and greater variability across samples. This indicates that, while the 0.45 μm filters recover communities with overall higher alpha diversity, the 0.22 μm filters show more variation in diversity among replicates.

The site-specific analysis (Figure 4b) further highlights significant differences among the Shannon indices, measured at NATS, CHIN, and CHOU, between the filter types (Kruskal-Wallis, $p < 0.05$). In NATS, the 0.45 μm filter retrieved a higher Shannon index, indicating a more diverse microbial community when using the larger pore size. In CHIN, the disparity was the most pronounced, with the 0.22 μm filter capturing significantly lower diversity compared to the 0.45 μm filter. In CHOU, the 0.22 μm filter exhibited the lowest Shannon index, with a narrow distribution, whereas the 0.45 μm filter captured a substantially more diverse community. Conversely, in ARTS, while the 0.45 μm filter showed slightly higher Shannon index values, the variability in diversity across samples made the difference statistically nonsignificant. In fact, the 0.45 μm plot is substantially overlapping with the 0.22 μm one.

The results of the alpha diversity analysis, based on the Shannon index and tested using the Kruskal–Wallis test, provide additional information with respect to the PERMANOVA analysis. At the CHOU site, alpha diversity was significantly different

between filters with different pore sizes, despite PERMANOVA not showing significant differences in community composition. Conversely, at the ARTS site, PERMANOVA detected significant differences between the filters, whereas the Kruskal-Wallis test showed no significant difference in the Shannon index values, indicating that compositional changes were not accompanied by diversity changes.

4 | Discussion

This study shows that microbial community composition is shaped by environmental context, but at the same time, its detection could be affected by the filter pore size used. As expected, site-specific conditions had the strongest effect, reflecting the known influence of local physicochemical factors, hydrodynamics, and nutrient availability in aquatic ecosystems (Zinger et al. 2011). Still, pore size also significantly influenced community detection, confirming that filter selection affects biodiversity detection (Galachyants et al. 2024). The differences found in the sampling sites considered suggest that, while both 0.22 μm and 0.45 μm filters effectively capture microbial diversity, their relative performance depends more on environmental context than on their intrinsic differences. These findings are particularly relevant for methodological standardization in eDNA research, emphasizing that filter selection should be adapted to the specific ecosystem and research objectives (Deiner et al. 2017). In line with this, the extraction kit effect was statistically significant in one site, but explained only a small fraction of the variance, and the main conclusions remained consistent across both methods. The divergence observed at the CHOU site suggests that differences due to extraction may occur depending on the monitored environment. Therefore, when no prior information on the sampling site is available, the extraction method should be carefully assessed through a pilot experiment.

4.1 | Quantitative and Qualitative Differences in Taxa Detection

Although a substantial portion of the microbial community was consistently detected across all samples, each filter type also captured a distinct subset of ASVs. Across the entire dataset, both pore sizes shared a large ASV core, yet the 0.45 μm pore size filter consistently recovered more unique ASVs than the 0.22 μm one. In site-specific analyses, the 0.45 μm pore size filter outperformed the 0.22 μm one in three of the four sites, highlighting its broader taxonomic retention. The consistent increase in the detection of some specific phyla using specific filters at different sites suggests that pore size may influence the selection of phyla based on their morphological or ecological characteristics within such environments. For instance, with the 0.45 μm pore size filter *Fibrobacterota*—cellulose degraders linked to plant fibers—were more frequently detected in both salt marsh sites. Similarly, *Planctomycetota*—known to colonize organic particles in aquatic environments—were also more frequently detected in CHIN.

Other groups instead were mostly detected at a given site, with no significant differences between smaller and larger pore size filters within that site, likely reflecting the environmental features of that location. For example, the higher abundance of *Cyanobacteria* in CHIN compared to the other sites, also when considering both filters, reflects their well-known dominance in dynamic, light-exposed environments (Paerl and Otten 2013), and is possibly due to the naturally greater presence of Cyanobacteria at this site. This finding may suggest that, in the case of a phylum that is particularly abundant at a site due to environmental conditions, it can be detected regardless of the filter type used.

Other examples are *Verrucomicrobiota* and *Planctomycetota*—both involved in polysaccharide degradation—that were found in varying proportions across sites, with higher relative abundances in some samples from ARTS. These expected patterns suggest that local conditions may shape the microbial community detected, rather than filter pore size being the only factor influencing what is retained.

However, as highlighted in Figure 2e, relevant differences emerge for specific taxa. *Bacteroidota* was better retained by the 0.45 μm filter, supporting previous findings that particle-attached microbes are more abundant in deeper waters, where sediment resuspension and organic aggregates play a key role in shaping microbial communities (Roth Rosenberg et al. 2021). In such conditions, the 0.45 μm filter appears more effective for capturing particle-associated taxa. Conversely, *Proteobacteria* tended to be relatively more represented with the 0.22 μm filter across all sites, with the strongest difference observed at CHOU and a similar but less pronounced pattern in the other locations. Furthermore, the 0.45 μm filter provided more consistent community profiles across replicates, while the 0.22 μm filter showed greater variability, as supported by the multivariate dispersion test. Therefore, in CHOU-like environments, the 0.22 μm filter may be preferable when targeting *Proteobacteria* specifically, whereas the 0.45 μm filter is more suitable for detecting particle-associated groups such as *Bacteroidota*.

A similar pattern can be observed in the case of *Verrucomicrobiota* and *Planctomycetota*, which were differently detected by the two pore sizes depending on the site, possibly due to site-specific environmental factors. These phyla, which are often linked to polysaccharide degradation, were detected in varying proportions across sites, with higher relative abundances in some samples from ARTS. These trends suggest that local differences in organic matter availability and hydrodynamic conditions may influence the retention of specific microbial groups, rather than filter pore size acting as a uniform selection mechanism. A different pattern, highlighted by both the Venn diagram and the heatmap, is that in the marsh sites—characterized by shallower waters and higher nutrient concentrations—there is a strong fluctuation in the detection of phyla depending on the filter used, especially in the artificial salt marsh (ARTS). Even though a presence/absence analysis might have suggested similar community structures between filters, relative abundance data reveal substantial differences. In fact, phyla such as *Campylobacterota* and *Fusobacteriota* were better detected with the 0.22 μm filter, while *Fibrobacterota* and *Nanoarchaeota* were more effectively captured with the 0.45 μm filter in both marsh sites. Interestingly, the detection of these specific phyla showed

no variation in abundance between filters in the deeper sites (CHIN and CHOU).

4.2 | Microbial Genera Driving Filter-Specific Community Composition

The differences in community composition observed across sites confirm that site-specific environmental conditions are the main drivers shaping microbial communities. The influence of local factors—such as hydrodynamics, availability of organic matter, and the degree of particle association—is especially evident in coastal habitats, where these parameters can vary greatly between sites (Alvisi et al. 2019). This is reflected in the marked separation of CHIN and CHOU samples by filter type, compared to the more similar profiles seen at the other sites. In fact, the effects were less pronounced in ARTS and NATS filters, which could indicate a more homogeneous microbial size distribution in these environments or a weaker partitioning between particle-attached and free-living microbial fractions. This pattern has been observed in estuarine and lagoon ecosystems (Xian et al. 2024), and is reflected in similar detection results for both types of filters. At the CHOU site, PCoA samples are well separated by filter type along the first principal component, which explains nearly 60% of the total variability, and most of the genera driving this separation, as indicated by the vector arrows, belong to the phylum *Bacteroidota*. This is coherent with what was observed in the previous heatmap (Figure 2b), in which this phylum was detected only with the 0.45 μm filters. In contrast, in the marsh sites, although the genera most strongly associated with filter differences in the PCoA still belong to *Bacteroidota*, these differences are less evident when looking at relative abundances in the heatmap. As a result, the separation between filters is less evident in these sites. A different pattern is observed in CHIN, which shows the strongest separation between filters. In this site's PCoA, samples are clearly divided along PC1—explaining 74% of the variance—and this is consistent with the PERMANOVA results, where the variable "pore" accounts for 72% of the variation. Among all sites, CHIN also has the lowest proportion of shared taxa between filters and the highest number of filter-specific taxa, reinforcing the observed separation. Interestingly, although the PCoA shows a clear separation between filters—mainly driven by genera belonging to the phylum *Bacteroidota*—the heatmap does not show a major difference in the overall abundance of this phylum between filters. This apparent contradiction is explained by differences at finer taxonomic resolution: while the total amount of *Bacteroidota* remains similar, the specific genera detected vary between filters. These shifts at the genus level are sufficient to cause the separation observed in the PCoA, emphasizing the need for high-resolution analyses when comparing microbial communities.

Despite the predominant influence of site-specific factors, the association of specific genera with filters of different pore sizes observed in the PCoA suggests that microbial taxa, independently of the site of detection, differ in their likelihood of being retained based on cell size, aggregation tendencies, or ecological niche preferences. In fact, we observed a consistent pattern across all the sites: the *NS5 marine group* was predominantly detected with the 0.45 μm filter, whereas the *NS3a marine group* and the *NS11-12 marine group* were primarily captured by the 0.22 μm filter. This may suggest that these taxa differ in their degree of association with particulate matter, affecting their retention due to different filter pore sizes. The *NS5 marine group* has been reported as predominantly free-living (Priest et al. 2022), but it is often associated with phytoplankton blooms, and it is characterized by the presence of genes for alginate degradation (Thomas et al. 2021; Wang et al. 2024). This suggests that, under bloom conditions, the *NS5 marine group* cells may be temporarily associated with algal-derived particles and could then explain why it was better retained in the wider pore filter in our study. Indeed, the degree of association with particulate matter could also explain the abundance in the wider pore filter of *Glaciecola*, a well-known bloom-associated, particle-attached bacterium (Wang et al. 2024), at the CHIN site. On the other hand, the *NS3a marine group*, coherently with its preferential retention by finer filters, has been described in the free-living fraction (Teeling et al. 2016), although specific studies on their ecology are still lacking. Finally, the *NS11-12 marine group* has been identified once in the "large" fraction of microbial communities (Morency et al. 2022), but its ecological role remains largely unresolved, indicating the need for further studies to resolve this apparent contradiction.

4.3 | Within-Sample Diversity Across Filter Types

To complement the community-level comparisons, alpha diversity was evaluated to assess whether filter type also influenced within-sample diversity. While previous analyses focused on taxonomic composition and the presence of shared or unique taxa, alpha diversity provides insights into richness and evenness, offering a more complete picture of potential biases introduced by pore size. In our study, 0.45 μm filters consistently yielded higher alpha diversity values, calculated as Shannon indices, than the 0.22 μm ones across all sites, with statistical significance in three out of four cases. The strongest effect was observed in CHIN and CHOU, where the 0.22 μm filter recovered the lowest microbial diversity, while the 0.45 μm filter retained a more diverse community. These sites are the deepest ones and are located closer to the open sea, where stronger hydrodynamics likely enhance sediment resuspension and organic matter aggregation. These conditions may promote the dominance of particle-associated microbes (Che et al. 2024), which have been reported to be better retained by larger pore size, as seen in studies employing sequential filtration strategies, where water is first passed through a larger filter to capture larger, particle-attached cells, and subsequently through a 0.22 μm filter to collect smaller, free-living microbes (Mestre et al. 2017; Padilla et al. 2015). Although our study used independent, non-sequential filtrations, the broader alpha diversity retained by the "medium size" 0.45 μm filter likely reflects its ability to capture both fractions in a single step. In contrast, 0.22 μm filters may underestimate diversity because of clogging, which can reduce filtration efficiency and retention capacity. Interestingly, in CHOU, the multivariate analysis did not identify pore size as a significant factor in overall community composition, yet the Shannon index revealed a clear difference in alpha diversity. This apparent discrepancy highlights the importance of using multiple diversity metrics: while PERMANOVA detects shifts in community composition based on relative abundance, it may

overlook changes in richness and evenness when dominant taxa remain similar. Both filters likely recovered a shared set of dominant taxa in CHOU, yielding similar overall profiles. However, the 0.45 μm filter captured additional rare taxa, thereby increasing richness and producing a more balanced distribution without altering the community's dominant structure. In contrast, at ARTS and NATS, where higher nutrient concentrations and turbulence may balance the proportion of free-living and particle-attached microbes, differences in alpha diversity between filters were less pronounced. This is particularly evident in ARTS, where no significant difference in Shannon diversity was observed, suggesting that filter-related differences mainly reflect shifts in dominant community composition rather than changes in overall richness or evenness. Across all sites, however, the consistent recovery of a higher number of ASVs with the 0.45 μm filter supports its suitability for metabarcoding studies focused on alpha diversity. Since both free-living and particle-attached bacteria play essential ecological roles, the ability of the 0.45 μm filter to capture taxa from both fractions makes it a valuable tool for eDNA studies, especially in heterogeneous aquatic environments.

5 | Conclusion

This study demonstrates that filter pore size has a clear impact on microbial community composition, with both 0.22 μm and 0.45 μm filters detecting a shared core of taxa but also recovering distinct community fractions. Across all sites, the 0.45 μm filter consistently retrieved a higher number of taxa and greater alpha diversity, indicating not only the absence of information loss but an actual gain in diversity compared to the 0.22 μm filter, highlighting its capacity to capture both free-living and particle-associated microbes. Importantly, the effect of pore size was modulated by site-specific environmental conditions, such as hydrodynamics and organic matter availability. This suggests that filter selection should be based not only on methodological consistency, but also on the ecological characteristics of the system and the target microbial groups. In fact, some phyla are more efficiently retained in certain environments, reinforcing the need for a flexible and informed approach to study design. Given these results, the 0.45 μm filter emerges as a powerful tool for holistic biodiversity assessments, and its ability to simultaneously recover microbial and eukaryotic eDNA opens new opportunities for integrated monitoring programs that are more cost-effective and scalable. In the context of large-scale and long-term ecological monitoring, where logistical efficiency and broad taxonomic coverage are essential, adopting a unified filtration approach using the 0.45 μm filter could enhance data comparability, reduce processing time, and support more comprehensive biodiversity in marine ecosystems.

Author Contributions

I.G. (Irene Gregori) contributed to the conception and design of the study, data acquisition and analysis, and wrote the original draft. F.M. (Francesco Martino) contributed to data acquisition and analysis and revised the manuscript. L.Z. (Lorenzo Zane) contributed to the conception and design of the study, provided supervision and funding, and revised the manuscript. A.P. (Alberto Pallavicini) contributed to study design, data analysis, visualization, and manuscript revision. A.V. (Alessandro Vezzi) contributed to the conception and design of the study, provided supervision and funding, and revised the manuscript.

Acknowledgments

This work was funded by the National Recovery and Resilience Plan (NRRP), Mission 4. Component 2 Investment 1.4—Call for tender No. 3138 of December 16, 2021, rectified by Decree n.3175 of December 18, 2021, of the Italian Ministry of University and Research, funded by the European Union–NextGenerationEU (Award Number: Project code CN_00000033, Concession Decree No. 1034 of 17 June 2022. Adopted by the Italian Ministry of University and Research, CUP C93C22002810006, Project title "National Biodiversity Future Center—NBFC,") which supported A.V. and L.Z. and funded I.G. PhD fellowship. L.Z. is also supported by the Italian Ministry of University and Research within the scientific research program of national interest "Preserving coastal marine ecosystem functions and services under climate change pressure and overfishing" (PRIN 2020 Prot. 2020J3W3WC), which also funded F.M. PhD fellowship. A.P. is supported by Interconnected Nord-Est Innovation Ecosystem (iNEST) and received funding from the European Union NextGenerationEU (PNRR—Mission 4 Component 2 Investment 1.5—D.D. 1058 23/06/2022, ECS_00000043). We thank Prof. Alberto Barausse (University of Padova) for his support in the fieldwork and assistance with sample collection. We also thank all the participants in the NBFC eDNA metabarcoding working group for the vibrant discussions and for their valuable insights. Open access publishing facilitated by Universita degli Studi di Padova, as part of the Wiley - CRUI-CARE agreement.

Ethics Statement

The authors have nothing to report.

Conflicts of Interest

The authors declare no conflicts of interest.

Data Availability Statement

The raw data underlying this study will be made available, upon acceptance of the manuscript, on the public online repository Sequence Read Archive (SRA) at NCBI, with BioProject accession number PRJNA1354795.

References

Aglieri, G., C. Baillie, S. Mariani, et al. 2021. "Environmental DNA Effectively Captures Functional Diversity of Coastal Fish Communities." *Molecular Ecology* 30, no. 13: 3127–3139. https://doi.org/10.1111/mec.15661.

Alvisi, F., T. Cibic, S. Fazi, L. Bongiorni, F. Relitti, and P. Del Negro. 2019. "Role of Depositional Dynamics and Riverine Input in Shaping Microbial Benthic Community Structure of Po Prodelta System (NW Adriatic, Italy)." *Estuarine, Coastal and Shelf Science* 227: 106305. https://doi.org/10.1016/j.ecss.2019.106305.

Anderson, M. J. 2006. "Distance-Based Tests for Homogeneity of Multivariate Dispersions." *Biometrics* 62, no. 1: 245–253.

Andrews, S. 2010. "FastQC: A Quality Control Tool for High Throughput Sequence Data [Online]." http://www.bioinformatics.babraham.ac.uk/projects/fastqc/.

Blabolil, P., L. R. Harper, Š. Říčanová, et al. 2021. "Environmental DNA Metabarcoding Uncovers Environmental Correlates of Fish Communities in Spatially Heterogeneous Freshwater Habitats." *Ecological Indicators* 126: 107698. https://doi.org/10.1016/j.ecolind.2021.107698.

Bohmann, K., A. Evans, M. T. P. Gilbert, et al. 2014. "Environmental DNA for Wildlife Biology and Biodiversity Monitoring." *Trends in Ecology & Evolution* 29, no. 6: 358–367. https://doi.org/10.1016/j.tree.2014.04.003.

Bolyen, E., J. R. Rideout, M. R. Dillon, et al. 2019. "Reproducible, Interactive, Scalable and Extensible Microbiome Data Science Using QIIME 2." *Nature Biotechnology* 37, no. 8: 852–857. https://doi.org/10.1038/s41587-019-0209-9.

Brandt, M. I., F. Pradillon, B. Trouche, et al. 2021. "Evaluating Sediment and Water Sampling Methods for the Estimation of Deep-Sea Biodiversity Using Environmental DNA." *Scientific Reports* 11, no. 1: 7856. https://doi.org/10.1038/s41598-021-86396-8.

Callahan, B. J., P. J. McMurdie, M. J. Rosen, A. W. Han, A. J. A. Johnson, and S. P. Holmes. 2016. "DADA2: High-Resolution Sample Inference From Illumina Amplicon Data." *Nature Methods* 13, no. 7: 581–583. https://doi.org/10.1038/nmeth.3869.

Cananzi, G., I. Gregori, F. Martino, et al. 2022. "Environmental DNA Metabarcoding Reveals Spatial and Seasonal Patterns in the Fish Community in the Venice Lagoon." *Frontiers in Marine Science* 9: 1009490. https://doi.org/10.3389/fmars.2022.1009490.

Carmona, R., R. Muñoz, and F. X. Niell. 2021. "Differential Nutrient Uptake by Saltmarsh Plants Is Modified by Increasing Salinity." *Frontiers in Plant Science* 12: 709453. https://doi.org/10.3389/fpls.2021.709453.

Chao, A., N. J. Gotelli, T. C. Hsieh, et al. 2014. "Rarefaction and Extrapolation With Hill Numbers: A Framework for Sampling and Estimation in Species Diversity Studies." *Ecological Monographs* 84: 45–67. https://doi.org/10.1890/13-0133.1.

Che, Y., C. Lin, S. Li, et al. 2024. "Influences of Hydrodynamics on Microbial Community Assembly and Organic Carbon Composition of Resuspended Sediments in Shallow Marginal Seas." *Water Research* 248: 120882. https://doi.org/10.1016/j.watres.2023.120882.

Chen, H., and P. C. Boutros. 2011. "VennDiagram: A Package for the Generation of Highly-Customizable Venn and Euler Diagrams in R." *BMC Bioinformatics* 12, no. 1: 35. https://doi.org/10.1186/1471-2105-12-35.

Coble, A. A., C. A. Flinders, J. A. Homyack, B. E. Penaluna, R. C. Cronn, and K. Weitemier. 2019. "eDNA as a Tool for Identifying Freshwater Species in Sustainable Forestry: A Critical Review and Potential Future Applications." *Science of the Total Environment* 649: 1157–1170. https://doi.org/10.1016/j.scitotenv.2018.08.370.

Collins, R. A., C. Baillie, N. C. Halliday, et al. 2022. "Reproduction Influences Seasonal eDNA Variation in a Temperate Marine Fish Community." *Limnology and Oceanography Letters* 7, no. 5: 443–449. https://doi.org/10.1002/lol2.10271.

Cook, L. S. J., A. G. Briscoe, V. G. Fonseca, J. Boenigk, G. Woodward, and D. Bass. 2025. "Microbial, Holobiont, and Tree of Life eDNA/eRNA for Enhanced Ecological Assessment." *Trends in Microbiology* 33, no. 1: 48–65. https://doi.org/10.1016/j.tim.2024.07.003.

Deiner, K., H. M. Bik, E. Mächler, et al. 2017. "Environmental DNA Metabarcoding: Transforming How we Survey Animal and Plant Communities." *Molecular Ecology* 26, no. 21: 5872–5895. https://doi.org/10.1111/mec.14350.

Djurhuus, A., C. J. Closek, R. P. Kelly, et al. 2020. "Environmental DNA Reveals Seasonal Shifts and Potential Interactions in a Marine Community." *Nature Communications* 11, no. 1: 254. https://doi.org/10.1038/s41467-019-14105-1.

Fediajevaite, J., V. Priestley, R. Arnold, and V. Savolainen. 2021. "Meta-Analysis Shows That Environmental DNA Outperforms Traditional Surveys, but Warrants Better Reporting Standards." *Ecology and Evolution* 11, no. 9: 4803–4815. https://doi.org/10.1002/ece3.7382.

Ficetola, G. F., C. Miaud, F. Pompanon, and P. Taberlet. 2008. "Species Detection Using Environmental DNA From Water Samples." *Biology Letters* 4, no. 4: 423–425. https://doi.org/10.1098/rsbl.2008.0118.

Ficetola, G. F., and P. Taberlet. 2023. "Towards Exhaustive Community Ecology via DNA Metabarcoding." *Molecular Ecology* 32, no. 23: 6320–6329. https://doi.org/10.1111/mec.16881.

Fu, M., L. Hemery, and N. Sather. 2021. "Cost Efficiency of Environmental DNA as Compared to Conventional Methods for Biodiversity Monitoring Purposes at Marine Energy Sites." https://doi.org/10.2172/1984522.

Galachyants, Y. P., Limnological Institute, Siberian Branch of the Russian Academy of Sciences, 3 Ulan-Batorskaya Str., Irkutsk, 664033, Russia, A. V. Bolbat, et al. 2024. "Test of Two Membrane Filter Types for Biomass Collection in Community Profiling by Metabarcoding." *Limnology and Freshwater Biology* 4: 888–899. https://doi.org/10.31951/2658-3518-2024-A-4-888.

Galand, P. E., O. Pereira, C. Hochart, J. C. Auguet, and D. Debroas. 2018. "A Strong Link Between Marine Microbial Community Composition and Function Challenges the Idea of Functional Redundancy." *ISME Journal* 12, no. 10: 2470–2478. https://doi.org/10.1038/s41396-018-0158-1.

Gifford, S. M., S. Sharma, J. M. Rinta-Kanto, and M. A. Moran. 2011. "Quantitative Analysis of a Deeply Sequenced Marine Microbial Metatranscriptome." *ISME Journal* 5, no. 3: 461–472. https://doi.org/10.1038/ismej.2010.141.

Goldberg, C. S., C. R. Turner, K. Deiner, et al. 2016. "Critical Considerations for the Application of Environmental DNA Methods to Detect Aquatic Species." *Methods in Ecology and Evolution* 7, no. 11: 1299–1307. https://doi.org/10.1111/2041-210X.12595.

Gómez-Rubio, V. 2017. "Ggplot2 - Elegant Graphics for Data Analysis (2nd Edition)." *Journal of Statistical Software* 77, no. 2: b02. https://doi.org/10.18637/jss.v077.b02.

He, X., N. W. Jeffery, R. R. E. Stanley, et al. 2023. "eDNA Metabarcoding Enriches Traditional Trawl Survey Data for Monitoring Biodiversity in the Marine Environment." *ICES Journal of Marine Science* 80, no. 5: 1529–1538. https://doi.org/10.1093/icesjms/fsad083.

Hering, D., A. Borja, J. I. Jones, et al. 2018. "Implementation Options for DNA-Based Identification Into Ecological Status Assessment Under the European Water Framework Directive." *Water Research* 138: 192–205. https://doi.org/10.1016/j.watres.2018.03.003.

Hsieh, T. C., K. H. Ma, and A. Chao. 2016. "iNEXT: An R Package for Interpolation and Extrapolation of Species Diversity (Hill Numbers)." *Methods in Ecology and Evolution* 7: 1451–1456. https://doi.org/10.1111/2041-210X.12613.

Illumina. 2013. "16S Metagenomic Sequencing Library Preparation. Preparing 16S Ribosomal RNA Gene Amplicons for the Illumina MiSeq System, 1, 28,".

Klymus, K. E., N. T. Marshall, C. A. Stepien, and Hideyuki Doi. 2017. "Environmental DNA (eDNA) Metabarcoding Assays to Detect Invasive Invertebrate Species in the Great Lakes." *PLoS One* 12, no. 5: e0177643. https://doi.org/10.1371/journal.pone.0177643.

Kolde, R., and M. R. Kolde. 2015. "Package 'Pheatmap'." *R Package* 1, no. 7: 790.

Martin, M. 2011. "Cutadapt Removes Adapter Sequences From High-Throughput Sequencing Reads." *EMBnet.Journal* 17, no. 1: 10. https://doi.org/10.14806/ej.17.1.200.

Martino, F., G. Cananzi, I. Gregori, et al. 2025. "Linking Water to the Bottom: eDNA Study of Benthic Invertebrates and Invasive Species in the Venice Lagoon." *Environmental DNA* 7, no. 2: e70093. https://doi.org/10.1002/edn3.70093.

McKnight, D. T., R. Huerlimann, D. S. Bower, L. Schwarzkopf, R. A. Alford, and K. R. Zenger. 2019. "Methods for Normalizing Microbiome Data: An Ecological Perspective." *Methods in Ecology and Evolution* 10: 389–400. https://doi.org/10.1111/2041-210X.13115.

McMurdie, P. J., and S. Holmes. 2013. "Phyloseq: An R Package for Reproducible Interactive Analysis and Graphics of Microbiome Census Data." *PLoS One* 8, no. 4: e61217. https://doi.org/10.1371/journal.pone.0061217.

Mestre, M., E. Borrull, M. M. Sala, and J. M. Gasol. 2017. "Patterns of Bacterial Diversity in the Marine Planktonic Particulate Matter Continuum." *ISME Journal* 11, no. 4: 999–1010. https://doi.org/10.1038/ismej.2016.166.

Miya, M. 2022. "Environmental DNA Metabarcoding: A Novel Method for Biodiversity Monitoring of Marine Fish Communities." *Annual Review of Marine Science* 14, no. 1: 161–185. https://doi.org/10.1146/annurev-marine-041421-082251.

Morency, C., L. Jacquemot, M. Potvin, and C. Lovejoy. 2022. "A Microbial Perspective on the Local Influence of Arctic Rivers and Estuaries on Hudson Bay (Canada)." *Elementa: Science of the Anthropocene* 10, no. 1: 00009. https://doi.org/10.1525/elementa.2021.00009.

Nguyen, B. N., E. W. Shen, J. Seemann, et al. 2020. "Environmental DNA Survey Captures Patterns of Fish and Invertebrate Diversity Across a Tropical Seascape." *Scientific Reports* 10, no. 1: 6729. https://doi.org/10.1038/s41598-020-63565-9.

Oksanen, J., G. L. Simpson, F. G. Blanchet, et al. 2001. "Vegan: Community Ecology Package." https://doi.org/10.32614/CRAN.package.vegan.

Olsen, G. J., D. J. Lane, S. J. Giovannoni, N. R. Pace, and D. A. Stahl. 1986. "Microbial Ecology and Evolution: A Ribosomal RNA Approach." *Annual Review of Microbiology* 40, no. 1: 337–365. https://doi.org/10.1146/annurev.mi.40.100186.002005.

Pace, N. R., D. A. Stahl, D. J. Lane, and G. J. Olsen. 1986. "The Analysis of Natural Microbial Populations by Ribosomal RNA Sequences." In *Advances in Microbial Ecology, Advances in Microbial Ecology*, edited by K. C. Marshall. Springer US. https://doi.org/10.1007/978-1-4757-0611-6_1.

Padilla, C. C., S. Ganesh, S. Gantt, et al. 2015. "Standard Filtration Practices May Significantly Distort Planktonic Microbial Diversity Estimates." *Frontiers in Microbiology* 6: 547. https://doi.org/10.3389/fmicb.2015.00547.

Paerl, H. W., and T. G. Otten. 2013. "Harmful Cyanobacterial Blooms: Causes, Consequences, and Controls." *Microbial Ecology* 65, no. 4: 995–1010. https://doi.org/10.1007/s00248-012-0159-y.

Parada, A. E., D. M. Needham, and J. A. Fuhrman. 2016. "Every Base Matters: Assessing Small Subunit rRNA Primers for Marine Microbiomes With Mock Communities, Time Series and Global Field Samples." *Environmental Microbiology* 18, no. 5: 1403–1414. https://doi.org/10.1111/1462-2920.13023.

Pinna, M., F. Zangaro, and V. Specchia. 2024. "Assessing Benthic Macroinvertebrate Communities' Spatial Heterogeneity in Mediterranean Transitional Waters Through eDNA Metabarcoding." *Scientific Reports* 14, no. 1: 17890. https://doi.org/10.1038/s41598-024-69043-w.

Pompanon, F., B. E. Deagle, W. O. C. Symondson, D. S. Brown, S. N. Jarman, and P. Taberlet. 2012. "Who Is Eating What: Diet Assessment Using Next Generation Sequencing." *Molecular Ecology* 21, no. 8: 1931–1950. https://doi.org/10.1111/j.1365-294X.2011.05403.x.

Priest, T., A. Heins, J. Harder, R. Amann, and B. M. Fuchs. 2022. "Niche Partitioning of the Ubiquitous and Ecologically Relevant NS5 Marine Group." *ISME Journal* 16, no. 6: 1570–1582. https://doi.org/10.1038/s41396-022-01209-8.

Quast, C., E. Pruesse, P. Yilmaz, et al. 2012. "The SILVA Ribosomal RNA Gene Database Project: Improved Data Processing and Web-Based Tools." *Nucleic Acids Research* 41, no. D1: D590–D596. https://doi.org/10.1093/nar/gks1219.

Roth Rosenberg, D., M. Markus Haber, J. Goldford, et al. 2021. "Particle-Associated and Free-Living Bacterial Communities in an Oligotrophic Sea Are Affected by Different Environmental Factors." *Environmental Microbiology* 23, no. 8: 4295–4308. https://doi.org/10.1111/1462-2920.15611.

Sønstebø, J. H., L. Gielly, A. K. Brysting, et al. 2010. "Using Next-Generation Sequencing for Molecular Reconstruction of Past Arctic Vegetation and Climate." *Molecular Ecology Resources* 10, no. 6: 1009–1018. https://doi.org/10.1111/j.1755-0998.2010.02855.x.

Taberlet, P. 2018. *Environmental DNA: For Biodiversity Research and Monitoring*. Oxford University Press.

Teeling, H., B. M. Fuchs, C. M. Bennke, et al. 2016. "Recurring Patterns in Bacterioplankton Dynamics During Coastal Spring Algae Blooms." *eLife* 5: e11888. https://doi.org/10.7554/eLife.11888.

Thomas, F., N. Le Duff, T.-D. Wu, et al. 2021. "Isotopic Tracing Reveals Single-Cell Assimilation of a Macroalgal Polysaccharide by a Few Marine Flavobacteria and Gammaproteobacteria." *ISME Journal* 15, no. 10: 3062–3075. https://doi.org/10.1038/s41396-021-00987-x.

Wang, F.-Q., D. Bartosik, C. Sidhu, et al. 2024. "Particle-Attached Bacteria Act as Gatekeepers in the Decomposition of Complex Phytoplankton Polysaccharides." *Microbiome* 12, no. 1: 32. https://doi.org/10.1186/s40168-024-01757-5.

Weiss, S., Z. Z. Xu, S. Peddada, et al. 2017. "Normalization and Microbial Differential Abundance Strategies Depend Upon Data Characteristics." *Microbiome* 5: 27. https://doi.org/10.1186/s40168-017-0237-y.

Xian, W. D., J. Ding, J. Chen, et al. 2024. "Distinct Assembly Processes Structure Planktonic Bacterial Communities Among Near- and Offshore Ecosystems in the Yangtze River Estuary." *Microbial Ecology* 87, no. 1: 42. https://doi.org/10.1007/s00248-024-02350-x.

Xu, X., Y. Yuan, Z. Wang, et al. 2023. "Environmental DNA Metabarcoding Reveals the Impacts of Anthropogenic Pollution on Multitrophic Aquatic Communities Across an Urban River of Western China." *Environmental Research* 216: 114512. https://doi.org/10.1016/j.envres.2022.114512.

Zhang, Y., M. Pavlovska, E. Stoica, et al. 2020. "Holistic Pelagic Biodiversity Monitoring of the Black Sea via eDNA Metabarcoding Approach: From Bacteria to Marine Mammals." *Environment International* 135: 105307. https://doi.org/10.1016/j.envint.2019.105307.

Zinger, L., L. A. Amaral-Zettler, J. A. Fuhrman, et al. 2011. "Global Patterns of Bacterial Beta-Diversity in Seafloor and Seawater Ecosystems." *PLoS One* 6, no. 9: e24570. https://doi.org/10.1371/journal.pone.0024570.

Supporting Information

Additional supporting information can be found online in the Supporting Information section. **Table S1:** Venice Lagoon Environmental Parameters. Annual ranges (min–max) of the values measured during 2023 by ARPAV (Agenzia Regionale per la Prevenzione e Protezione Ambientale del Veneto). Data reported are from the ARPAV closest sites to the Venice Lagoon sampling sites investigated in this study (NATS, ARTS, CHIN). The ARPAV code column lists the official identifiers of the ARPAV stations. Concentrations of Total Dissolved Nitrogen (TDN), Total Dissolved Phosphorus (TDP), and Total Suspended Solids (TSS) are available at https://www.arpa.veneto.it/dati-ambientali/open-data/file-e-allegati/soaml/laguna-di-venezia/tss-nutr-acqua. Salinity (Practical Salinity Units, PSU) values are available at https://www.arpa.veneto.it/dati-ambientali/open-data/file-e-allegati/soaml/laguna-di-venezia/dati-sonda. Data for the CHOU site are not included because comparable measurements were unavailable. **Table S2:** Details about the 48 considered samples. "*" Indicates samples have been excluded from the analysis due to insufficient sequencing depth, "**" indicates the ones sacrificed to maintain a balanced dataset between filter types. **Figure S1:** Rarefaction curves of microbial communities across samples. The number of detected ASVs is plotted against the sequencing depth, showing the accumulation of species with increasing sequencing effort. Each curve represents an individual sample, with labels indicating sample IDs. **Figure S2:** Overall Venn diagram showing the overlap of OTUs detected by 0.45 μm and 0.22 μm filters across all samples in the dataset. A total of 157 OTUs were shared between both filter types, while 91 and 64 OTUs were uniquely detected by

the 0.45 μm and 0.22 μm filters, respectively. **Figure S3:** Venn diagrams showing the overlap of OTUs detected by 0.45 μm and 0.22 μm filters across all samples, separated by extraction kit: (a) Blood & Tissue (bl&ti) and (b) PowerWater (powa). For bl&ti, 114 OTUs were shared between both filter types, while 73 and 58 OTUs were uniquely detected by the 0.45 μm and 0.22 μm filters, respectively. For powa, 106 OTUs were shared, with 73 and 42 OTUs uniquely detected by the 0.45 μm and 0.22 μm filters, respectively. In both cases, the 0.45 μm filter consistently recovered a higher number of unique taxa compared to the 0.22 μm filter, reflecting the same overall pattern observed in the complete dataset. **Figure S4:** Principal Coordinates Analysis (PCoA) based on Bray–Curtis dissimilarities showing microbial community composition across sites and extraction methods. Samples are colored by extraction method (blood&tissue in red, powerwater in blue), with lines connecting paired filters from the same water sample. Ellipses indicate the samples within each site (ARTS, CHIN, CHOU, NATS). The plots are separated by pore size filter: (a) 0.22 μm and (b) 0.45 μm. Among sites, CHOU was the only case where the extraction method significantly influenced community structure. **Figure S5:** Violin plots of Shannon diversity index comparing microbial diversity captured by 0.22 μm (light blue) and 0.45 μm (orange) filters within the two extraction kits: (a) Blood & Tissue and (b) PowerWater. The width of each violin represents the density distribution of Shannon index values, with wider sections indicating more frequent values. The boxplot inside the violin displays the interquartile range (IQR, 50% of the data), the horizontal line represents the median, and whiskers extend to the 95% confidence interval (95% CI) or 1.5×IQR from the quartiles. Significant differences ($p < 0.05$, Kruskal–Wallis test) are indicated by asterisks, with $^{**}p < 0.01$ and $^{***}p < 0.001$.